Journal of Alloys and Compounds 650 (2015) 393–398

Contents lists available at ScienceDirect

Journal of Alloys and Compounds

journal homepage: http://www.elsevier.com/locate/jalcom

Effects of micro arc oxidation on fatigue limits and fracture morphologies of 7475 high strength aluminum alloy

Kong Dejun [a, b, *], Liu Hao [a], Wang Jinchun [a]

[a] College of Mechanical Engineering, Changzhou University, Changzhou, 213164, PR China
[b] Jiangsu Key Laboratory of Materials Surface Science and Technology, Changzhou University, Changzhou, 213164, PR China

ARTICLE INFO

Article history:
Received 4 March 2015
Received in revised form
30 June 2015
Accepted 27 July 2015
Available online 30 July 2015

Keywords:
Micro arc oxidation (MAO)
Fatigue limit
Fracture morphology
Interface morphology
Residual stress

ABSTRACT

The oxide coatings with thicknesses of 8 μm, 10 μm, and 15 μm were prepared on 7475 aluminum alloy with micro arc oxidation (MAO) by controlling MAO time, the fatigue limits of original and MAO samples were contrastively measured by the Roccati method. The surface-interface morphologies, fracture morphologies, surface phases, and residual stresses of MAO coating were analyzed with a scanning electron microscopy (SEM), X-ray diffractometer (XRD) and XRD stress tester, respectively. The results show that fatigue limits of the MAO samples decreases as the coating thickness increasing. The fatigue limit of MAO sample with thickness of 8 μm, 10 μm, and 15 μm decreases by 6.48%, 8.33%, and 11.11%, respectively, compared with the original sample. The residual stress and defects introduced by MAO were the main factors of decreasing fatigue limits.

1. Introduction

As a series of Al–Zn–Mg–Cu aluminum alloy, 7475 aluminum alloy with light weight, high strength and excellent comprehensive performance has been widely used on various industrial fields, but there is still a low surface hardness, poor wear resistance and weak corrosion resistance and etc., and the failure of aluminum alloy often occurs on the material surface during service life. Therefore, the surface modification treatments such as anodic oxidation [1], rare earth conversion coating [2], ion implantation [3] and laser processing [4] are often adopted to improve its usage performance [5], which can effectively improve the fraction-wear and corrosion properties, but there are some disadvantages such as high energy consumption, complex processes and thin thickness, having greatly limited their usage [6]. The surface properties such as corrosion resistant property [7] and wear performance [8] of aluminum alloys can effectively be increased by MAO, which also has some unique advantages such as simple process, low cost, and environmental protective in comparison with that by the traditional methods [9]. The MAO can form a layer of oxide coating with the maximum thickness of 200 μm, however, the oxide coating with several micrometers is enough to protect the metal base, and the thicker oxide coating will inevitably increase power consumption and decrease the production efficiency of MAO. The literatures on fatigue behavior of MAO coatings are limited, Yerokhin [10] et al. studied fatigue properties of Mg alloy MAO coating with different thicknesses, which reported that MAO coatings reduced endurance limit of Mg alloy by no more than 10%. Kehan [11] et al. evaluated the residual stress attributed to the MAO coating of 6082 aluminum alloy by X-ray diffraction (XRD) method, which found that the stresses degraded the fatigue properties. Wen Lei [12] et al. made a study focused on the relationships between the coating microstructure and the fatigue property of the SMAT-MAO coated aluminum alloy, which confirmed that the structure defects can lead to an early fatigue crack initiation in the substrate and promote the propagation of cracks. Because the MAO may produce some surface defects and tensile residual stresses, which have a certain influence on the fatigue performance, the effects of MAO on fatigue property is rarely investigated, and the mechanism of oxide coating thickness on fatigue performance is not reported yet [10–12]. The MAO samples with thicknesses of 8 μm, 10 μm, and 15 μm were obtained by controlling of MAO time in this paper, the fatigue limits were tested by the Roccati fatigue method, and the fracture morphologies and phases of MAO coatings were analyzed with SEM (scanning electron microscopy), XRD (X-ray diffractometer), respectively, and the effects of MAO on fatigue strength of 7475

* Corresponding author. College of Mechanical Engineering, Changzhou University, Changzhou, 213164, PR China.
E-mail address: kong-dejun@163.com (K. Dejun).

http://dx.doi.org/10.1016/j.jallcom.2015.07.262
0925-8388/

aluminum alloy were researched, providing an experimental basis for MAO applying on aluminum alloy.

2. Experimental

The experimental material was 7475 aluminum alloy with the chemical compositions as follows (mass, %): Si ≤ 0.10, Fe ≤ 0.12, Mn ≤ 0.06, Cu 1.2–1.9, Mg 1.9–2.6, Cr 0.18–0.25, Ti ≤ 0.06, Zn 5.2–6.2, the remainder was Al. The processes of MAO were shown as follows: degreasing, water washing, MAO, water washing and drying. The conditions of MAO were shown as follows: alkaline electrolyte of Na_2SiO_3–KOH solution, temperature of 50 °C, positive/negative current density of 10 A/dm^2, frequency of 50 Hz, positive/negative ratio of 50%/50%, cooling way of circulating water, MAO time of 10 min, 15 min and 30 min, respectively, as a result, the required samples were gained. The fatigue limits of the samples before and after MAO were tested on a EHF-EG250KN-40L type fatigue test machine with the Roccati fatigue method, the size of fatigue sample was shown as Fig. 1. The surface-interface morphologies of MAO coating and fracture morphologies were observed with a JSM-6360LA type SEM (scanning electron microscopy), the phases and residual stresses of MAO coating were analyzed with a D/max2500 PC type XRD (X-ray diffractometer) and an X350-A type stress tester, respectively.

3. Analysis and discussion of results

3.1. Fatigue limits

3.1.1. Theoretical analysis

According to the Miner's linear cumulative damage theory, the fatigue damage D was defined as the ratio of cycle number n to fatigue life N under the certain stress, i.e.

$$D = n/N \tag{1}$$

Under the influence of multi-level stresses, the fatigue failure occurs when

$$\sum n_i/N_i = 1 \tag{2}$$

where n_i and N_i was the cycle number and fatigue life under stress level of i, respectively.

According to the Miner's fatigue damage rule, a way of interpolation was used to calculate fatigue limit σ_r with the support of fatigue damage number under step loading and similar material's fatigue curves, which was called the Roccati method [13].

3.1.2. Loading methods

The maximum tensile force $F_b = 9.662$ kN and fracture force $F_f = 7.861$ kN of the original sample were obtained from the static tensile curve, as shown in Fig. 2. The cross-section area of the original sample was 30 mm^2, while that of the fracture was 17.5 mm^2. Therefore, the tensile strength σ_b and fracture strength σ_f of the original sample was 322 MPa, and 450 MPa, respectively.

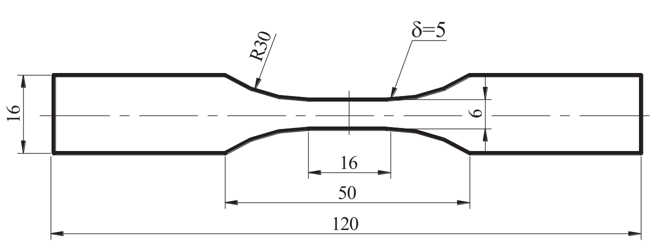

Fig. 1. Sketch of fatigue samples.

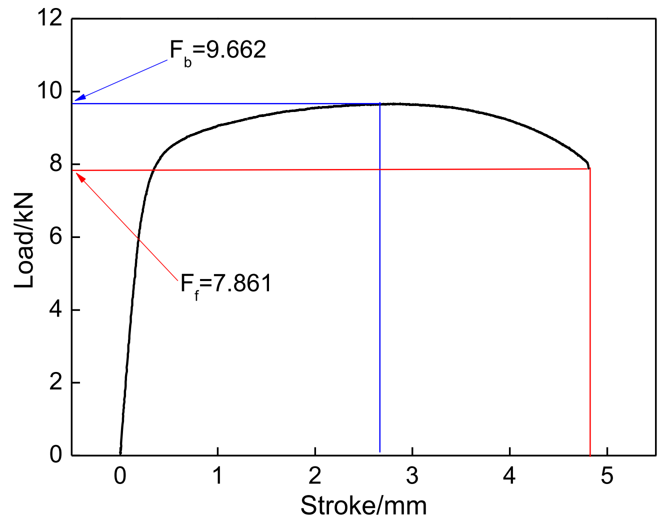

Fig. 2. Static tensile curve of original sample.

According to the relation between the fatigue limit and tensile property [14], the estimation equation of the Ding's fatigue limit [15] was

$$\sigma_{-1} = 0.19\sigma_f + 2 \tag{3}$$

$$\sigma_r = \{f + (1-f)[(1+r)/2]^n\}\sigma_b \tag{4}$$

where f was fatigue stress ratio; $f = \sigma_{-1}/\sigma_b$, σ_b was tensile strength; r was stress ratio; n was material constant, $n = 1/(cf)$; c was undetermined coefficient, for aluminum alloy, $c = 1.65$.

According to Eqs (3) and (4), the theoretical estimated fatigue limit of the original sample was 210 MPa. According to the Roccati fatigue test principle, the initial loading stress level should meet σ_0=(0.5–1)σ_r, as a result, the initial loading stress of the original sample was 130 MPa, and the initial loading stresses of MAO samples with thicknesses of 8 μm, 10 μm, and 15 μm were 130 MPa, 160 MPa, and 190 MPa, respectively. The loading stress increased 30 MPa every 2 × 10^4 cycles until the sample was broken, the loading processes were shown in Fig. 3.

3.1.3. Fatigue damage–stress curve

Based on the theoretical fatigue strength estimated by Eqs (1) and (2), three fatigue life curves with the fatigue limit of 175 MPa, 210 MPa, and 240 MPa was selected as reference curves. These curves were corresponded to the lowest, middle and highest position of estimated theoretical fatigue limit of the tested samples. The cumulative damage value n_i/N_i of each stress level was calculated in Table 1.

The cumulative damage–stress curves were shown in Fig. 4, the fatigue limit of the original sample was 216 MPa (Fig. 4(a)), while that of the MAO samples with thickness of 8 μm, 10 μm, and 15 μm was 202 MPa, 198 MPa, and 192 MPa (Fig. 4(b)), respectively, which decreased by 6.48%, 8.33%, and 11.11%, respectively, compared with that of the original sample, as a result, the fatigue limit decreased with the increase of the MAO coating thickness.

3.2. Morphologies of fatigue fractures

3.2.1. Morphologies of crack source zones

The fracture morphologies of MAO samples with different thickness were shown in Fig. 5. With the increase of MAO coating